Korean J. Chem. Eng., 33(3), 1070-1074 (2016)
DOI: 10.1007/s11814-015-0225-5

pISSN: 0256-1115
eISSN: 1975-7220

Enhanced moisture-barrier property and flexibility of zirconium oxide/polymer hybrid structures

Se Hee Lim, Seung-Woo Seo, Eun Jung, Heeyeop Chae, and Sung Min Cho†

School of Chemical Engineering, Sungkyunkwan University, Suwon 16419, Korea
(*Received 7 August 2015 • accepted 22 October 2015*)

Abstract−New zirconium oxide (ZrO_2)-based organic-inorganic multilayers were fabricated and tested for flexible moisture barriers and compared with typical aluminum oxide (Al_2O_3)-based multilayers. We report that amorphous ZrO_2 had a better intrinsic barrier property than that of amorphous Al_2O_3. Due to the lower elastic modulus of ZrO_2, the ZrO_2-based structures had better flexibility than that of the Al_2O_3-based structures. The ZrO_2-based barrier was superior to the Al_2O_3-based barrier not only for flexibility but also for barrier performance. The barrier property and flexibility of the ZrO_2-based structures were enhanced by about 20% and 30% over those of the Al_2O_3-based structures, respectively.

Keywords: Moisture Barrier, Atomic Layer Deposition, Aluminum Oxide, Zirconium Oxide

INTRODUCTION

Aluminum-oxide (Al_2O_3) thin films grown by atomic layer deposition (ALD) at a low temperature have been widely studied for a plastic-substrate moisture-barrier layer or a thin-film encapsulation layer of organic light-emitting diodes and organic photovoltaic cells. It is advantageous for the layer to have both high material density and low elastic modulus to achieve a flexible moisture-barrier with an ALD-grown metal-oxide layer. As density and elastic modulus are dependent on the material, it is important to select a proper material for the purpose. The elastic modulus of Al_2O_3 grown by ALD is 203 GPa [1], whereas that of ALD-grown zirconium oxide (ZrO_2) is about 100 GPa [2]. Thus, a ZrO_2 layer is expected to exhibit better flexibility than that of an Al_2O_3 layer with the same thickness. However, the ZrO_2 layer is prone to crystallize even at 50 °C [3], so its moisture barrier property becomes worse due to easier moisture diffusion through the grain boundaries. In contrast, an Al_2O_3 layer that stays amorphous at high temperature [4] has been considered as a better moisture-barrier layer. ZrO_2 crystallization has been reported in an Al_2O_3/ZrO_2 nanolaminate structure grown at 80 °C [5]. Another related study reported that crystallization began at a ZrO_2 thickness of about 4 nm [6]. There have been no detailed reports on intrinsic moisture-barrier property of amorphous ZrO_2 in comparison with amorphous Al_2O_3.

Organic/inorganic multilayer structures are commonly used as flexible moisture barriers [7-9]. Organic materials are rugged but highly permeable to moisture, whereas inorganic materials are almost impermeable to moisture but very fragile. The organic/inorganic multilayer approach seems to be the best practice to capitalize on the advantages of these materials. For example, the critical tensile strain of 20 nm-thick Al_2O_3 thin film grown using ALD on a polyethylene naphthalate (PEN) substrate is 1.2% [10], indicating that cracks could be generated upon tensile bending with a radius less than 5.2 mm. However, the critical bending radius could be reduced further [11] if the organic layers were incorporated into the Al_2O_3 layer, due to stress relaxation of the organic layers.

We report the moisture-barrier property and flexibility of ZrO_2-based organic/inorganic multilayer structures for the first time in direct comparison with the typical Al_2O_3-based structures. The moisture-barrier property was measured using electrical calcium (Ca) test at an accelerated condition of 85 °C and 85% relative humidity (RH). Flexibility was tested by measuring changes in the moisture-barrier property before and after 10,000 bending cycles with bending radii from 3-20 mm. We used a plasma-polymerized (PP) organic layer for the organic/inorganic multilayer structures, which can be grown in a plasma-enhanced chemical vapor deposition (PECVD) reactor with an organic monomer source.

EXPERIMENTAL PROCEDURE

In-house designed and built deposition equipment was used to deposit Al_2O_3 and ZrO_2 using ALD, with metal-organic precursors of trimethyl aluminum (TMA) and tetrakis (ethylmethylamino) zirconium (TEMAZ), which were vaporized at 5 °C and 30 °C, respectively. Water was used as the oxidant and vaporized at room temperature. Deposition was carried out at 80 °C. One Al_2O_3 or ZrO_2 growth cycle was subjected to TMA or TEMAZ injection for 2 s, purging with argon (Ar) for 10 s, water injection for 2 s, and purging for 10 s, respectively. One cycle produced 1.1 Å-thick Al_2O_3 or 0.9 Å-thick ZrO_2, on average, at that temperature. Hexane was introduced into the growth chamber with Ar carrier gas for PECVD of the PP. The plasma was ignited by an inductively coupled coil, connected to a radio-frequency power supply operated at 50 W. The growth rate of the optically transparent PP was 30 nm/min. We prepared six different multilayer moisture barrier structures using PEN substrate, composed of inorganic Al_2O_3 or ZrO_2

†To whom correspondence should be addressed.
E-mail: sungmcho@skku.edu

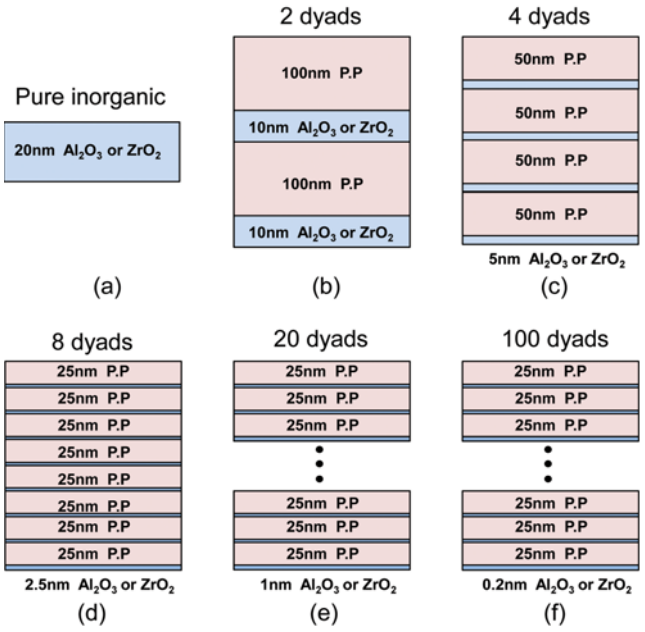

Fig. 1. Schematic diagrams of six different moisture-barrier structures. Here, P.P and dyad mean a plasma polymer layer and a period of P.P and Al_2O_3 (or ZrO_2) layers, respectively.

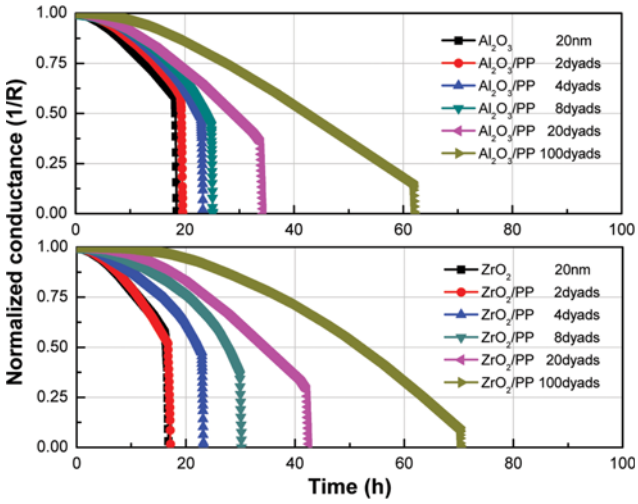

Fig. 3. Electrical Ca test results of Al_2O_3- and ZrO_2-based multilayer structures showing the electrical conductance of Ca decreasing with time. Measurement was carried out under 85 °C and 85% relative humidity condition.

and organic PP layers, as shown in Fig. 1. Due to the much poorer moisture-barrier property of the organic layer relative to the inorganic layer, the moisture-barrier property predominantly depends on the thickness of the inorganic layer. As all structures had the same total inorganic-layer thickness of 20 nm, they were expected to have a similar moisture-barrier property, even though the total thickness of the PP sub-layers was not the same for all structures. Unlike the ALD process, it was difficult to control thickness below 20 nm during PECVD for the PP, resulting in different total PP thicknesses for 20 and 100 dyads in Fig. 1. A structure with a higher number of dyads is expected to have better flexibility, as the thinner inorganic layer has a larger critical tensile strain [12]. In this regard, the structure (f) in Fig. 1 should show the best flexibility among all structures.

RESULTS AND DISCUSSION

We show actual transmission-electron-microscopic images of 100-dyad Al_2O_3 and PP multilayer structure in Fig. 2. The thickness of an Al_2O_3 layer in the multilayer structure is 2 Å, which is produced by 2 ALD cycles. The extremely thin Al_2O_3 layers separated by PP layers are continuous and can work for flexible moisture-barrier layers. Fig. 3 shows the electrical Ca test results of the upper Al_2O_3-based structures and the lower ZrO_2-based structures. As the normalized conductance of Ca (y-axis) decreases continuously from 1 (fresh Ca) to 0 (fully oxidized Ca) as time (x-axis) increases due to moisture permeating through the barrier, a structure with a longer elapsed time means a better moisture barrier. A detailed explanation of the electrical Ca test method can be found in the literature.[6] All measurements were at 85 °C and 85% RH. Because the ZrO_2 moisture-barrier property becomes poorer than that of Al_2O_3 beyond a thickness of about 4 nm as the ZrO_2

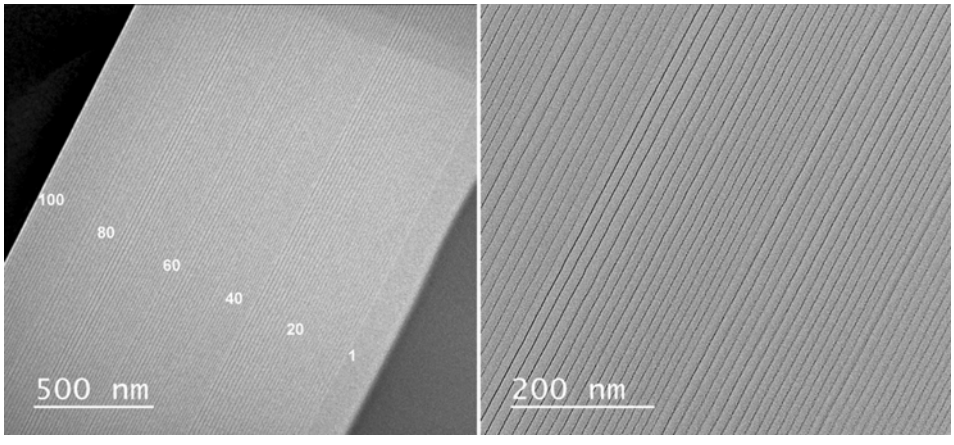

Fig. 2. Transmission electron microscopic images of 100 dyads composed of 2 Å Al_2O_3 and 20 nm plasma polymer layers.

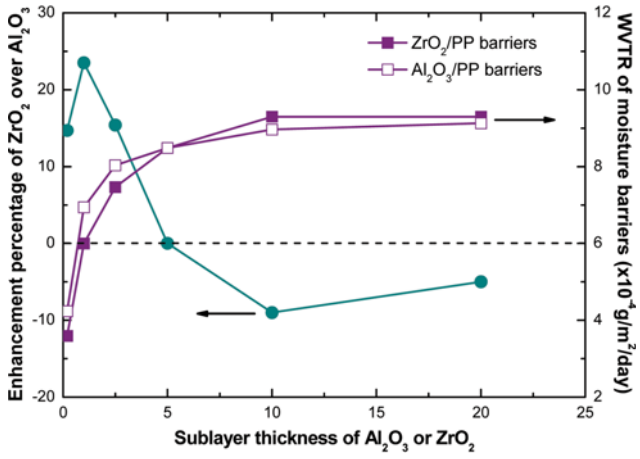

Fig. 4. Water vapor transmission rate and enhancement percentage of ZrO_2 over Al_2O_3 as a function of the sublayer thickness of Al_2O_3 or ZrO_2.

crystallizes [6], the moisture-barrier property of Al_2O_3- and ZrO_2-based structures was the reverse of the 4-dyad structure (5 nm-thick ZrO_2 sublayers) as the center. The barrier property of the Al_2O_3-based structures was better for a dyad number lower than 4, whereas that of ZrO_2-based structures was better for a dyad number higher than 4. As a result, a multilayer structure with a ZrO_2 sublayer thickness less than 5 nm shows a better moisture-barrier property, indicating that ZrO_2 is intrinsically a better moisture barrier than that of Al_2O_3 if it remains amorphous. In addition, a multilayer structure with a higher number of dyads has a better moisture-barrier property because including more PP layers creates a longer tortuous moisture path through the defects residing in the inorganic sublayers [13]. The 8-, 20-, and 100-dyad ZrO_2/PP barriers showed 15.4, 23.5, and 14.7% better barrier property than that of the corresponding Al_2O_3/PP barriers, respectively. The water vapor transmission rate (WVTR) of the 100-dyad ZrO_2/PP barrier was 3.6×10^{-4} g/m^2/day, and the WVTR of all barriers tested was about 10^{-4} g/m^2/day. The above discussion is summarized as a graph in Fig. 4. The moisture barrier property of the Al_2O_3- and ZrO_2-based barriers was reverse at a sublayer thickness of about 5 nm, and the WVTR was increased continuously as the sublayer thickness increased.

The electrical Ca test was carried out before and after 10,000 bending cycles at different bending radii to determine flexibility of the barriers (Fig. 5). As shown in Fig. 5(a) for Al_2O_3-based barriers, the moisture-barrier property degraded after the bending cycles, and the degradation became more severe at a smaller bending radius. The barrier property of the 20- and 100-dyad barriers remained unchanged down to a 10 mm bending radius, whereas that of the others decreased slightly, even at a relatively large bending radii. The slight reduction in the barrier property after the bending cycles was not due to cracks but fatigue exerted by the bending process. The barrier property was lost completely by reducing the bending radius to 5 mm, due to cracks generated during the bending cycles for barriers with number of dyads less than 20. However, the 20- and 100-dyad barriers still worked as a barrier but with a 32% and 21% reduced property, respectively. All

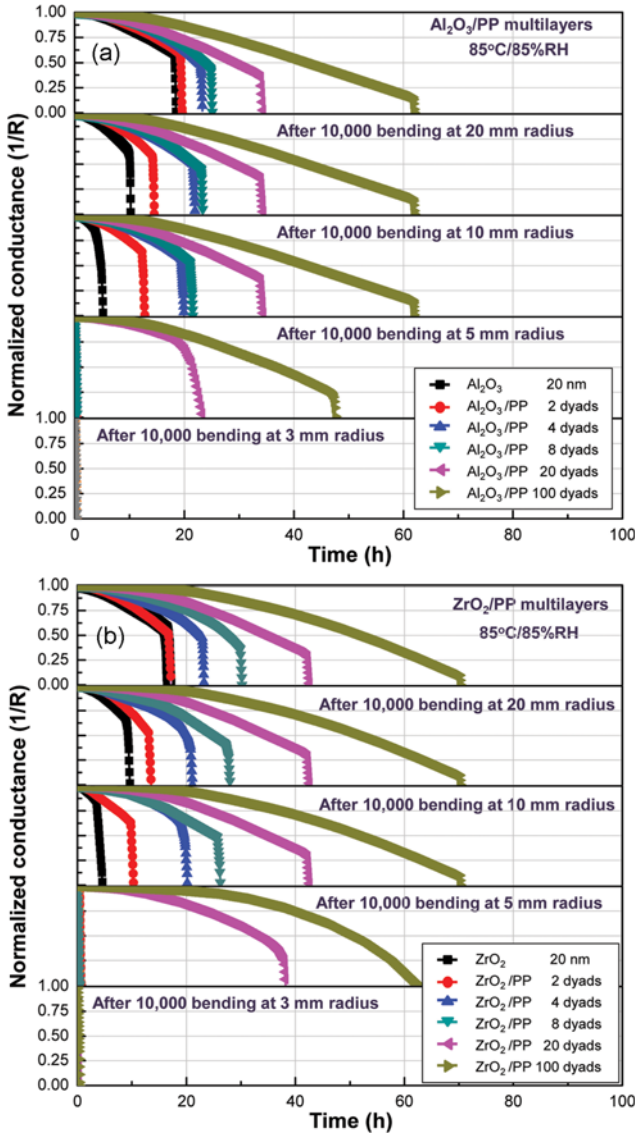

Fig. 5. Electrical Ca test results of (a) Al_2O_3-based multilayers and (b) ZrO_2-based multilayers before and after 10,000 bending cycles at different bending radii.

barriers lost their barrier property at the 3 mm bending radius.

The ZrO_2-based barriers showed a similar bending property to that of the Al_2O_3-based barriers (Fig. 5(b)). The 20- and 100-dyad ZrO_2/PP barriers degraded by only 9.5% and 11% after the bending cycles at a 5 mm bending radius, respectively, which was at least 50% less of the decreases in the corresponding Al_2O_3/PP barrier property during bending. Although the ZrO_2-based barriers also lost their property at the 3 mm bending radius, the ZrO_2-based barriers were more flexible than the Al_2O_3-based barriers. We put the 20- and 100-dyad Al_2O_3/PP, and ZrO_2/PP barriers into an approximately neutral plane by laminating PEN film onto the barrier structure using an ultraviolet curable resin to further investigate barrier flexibility. Because the bonding resin overlay the barrier structure, the barriers were not exactly in a neutral plane. Fig. 6 shows the Ca test result before and after 10,000 bending cycles at bending radii of 5 and 3 mm. As the barriers in a neutral plane were

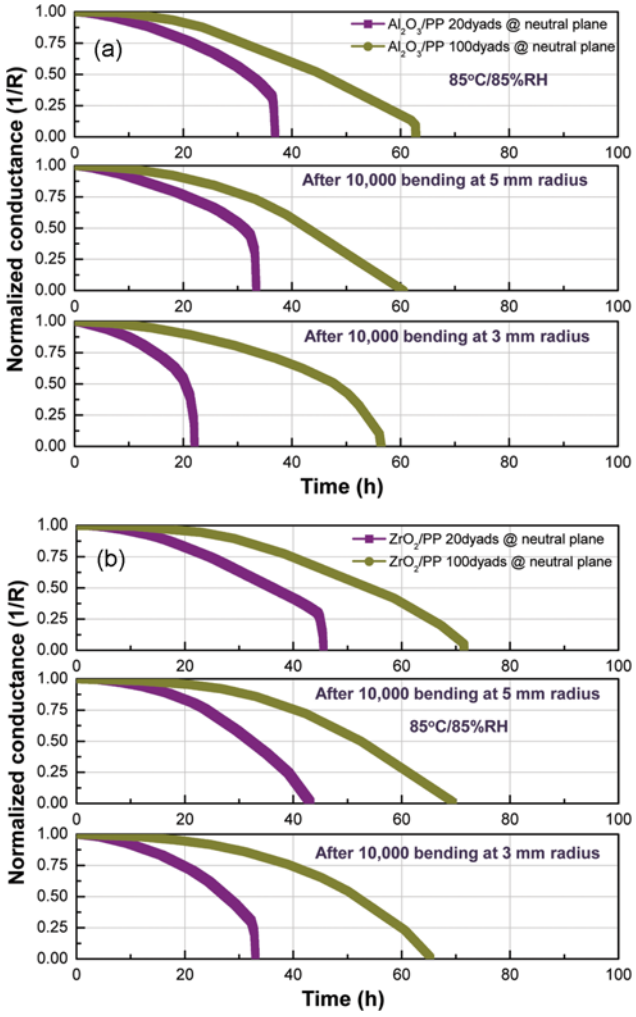

Fig. 6. Electrical Ca test results of (a) Al_2O_3-based multilayers and (b) ZrO_2-based multilayers in a neutral plane before and after 10,000 bending cycles at different bending radii.

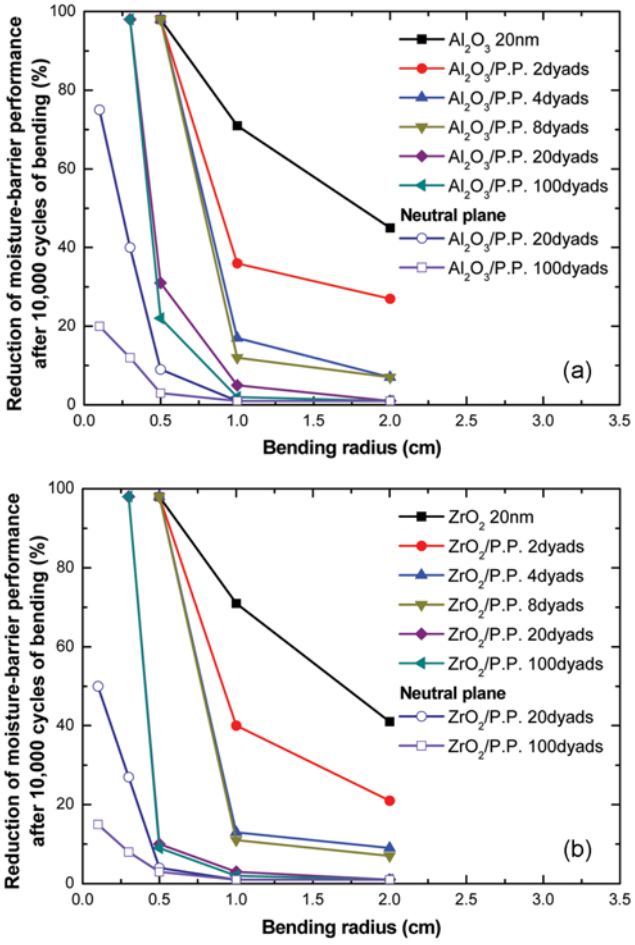

Fig. 7. Reduction percentage of moisture-barrier property of all the (a) Al_2O_3-based and (b) ZrO_2-based structures from their initial properties, after 10,000 bending cycles with various bending radii.

stress free, they did not crack, even at a 3 mm bending radius, even though the barrier property degraded. The percent degradation rates of the 20- and 100-dyad ZrO_2-based barriers were 27% and 8%, respectively, whereas those of the 20- and 100-dyad Al_2O_3-based barriers were 40% and 10%, respectively. Thus, it is clear that the ZrO_2-based barriers were more flexible than that of the Al_2O_3-based barriers. Additionally, the barriers with thinner inorganic sublayers showed better performance for the flexible moisture barrier.

Fig. 7 shows the percent reduction of moisture-barrier performance after 10,000 cycles of bending at different bending radii for all the Al_2O_3- and ZrO_2-based multilayer barrier structures. As discussed above, barriers in a neutral plane survive after 10,000 bending cycles at a 3 mm bending radius, while other barriers lose their barrier property. We further reduced the bending radius to 1 mm to compare the flexibility of Al_2O_3- and ZrO_2-based multilayer barriers in a neutral plane. The percent reduction of moisture-barrier performance of the 20- and 100-dyad ZrO_2-based barriers after the bending was 50% and 15%, respectively, whereas that of the 20- and 100-dyad Al_2O_3-based barriers was 75% and 20%, respectively. We think that the 100-dyad ZrO_2-based multilayer structure is the most flexible moisture barrier among all barrier structures utilizing inorganic layers reported so far. The flexible moisture barrier can be utilized as a thin-film encapsulation structure for foldable OLED displays.

CONCLUSIONS

We fabricated and tested typical Al_2O_3-based and new ZrO_2-based multilayer barriers for flexibility. Due to the lower elastic modulus of ZrO_2 than that of Al_2O_3, the ZrO_2-based barriers were more flexible experimentally than the Al_2O_3-based barriers, as expected in theory. The ZrO_2-based barrier was superior to the typical Al_2O_3-based barrier not only for flexibility but also for moisture-barrier performance. The barrier property of the ZrO_2-based barrier was about 20% better than that of the Al_2O_3-based barrier at an inorganic sublayer thickness less than 5 nm.

ACKNOWLEDGEMENTS

This study was supported by the National Research Foundation

of Korea (NRF) grant funded by the Korea government (MSIP) (NRF-2014R1A2A1A11052847).

REFERENCES

1. D. C. Miller, R. R. Foster, S.-H. Jen, J. A. Bertrand, S. J. Cunningham, A. S. Morris, Y.-C. Lee, S. M. George and M. L. Dunn, *Sensors and Actuators A: Physical*, **164**, 58 (2010).
2. B. H. Lee, V. R. Anderson and S. M. George, *Chem. Vap. Deposition*, **19**, 204 (2013).
3. D. M. Hausmann and R. G. Gordon, *J. Cryst. Growth*, **249**, 251 (2003).
4. L. Zhang, H. C. Jiang, C. Liu, J. W. Dong and P. Chow, *J. Phys. D: Appl. Phys.*, **40**, 3707 (2007).
5. J. Meyer, P. Gorrn, F. Bertram, S. Hamwi, T. Winkler, H.-H. Johannes, T. Weimann, P. Hinze, T. Riedl and W. Kowalsky, *Adv. Mater.*, **21**, 1845 (2009).
6. S.-W. Seo, E. Jung, H. Chae and S. M. Cho, *Org. Electron.*, **13**, 2346 (2012).
7. J. S. Lewis and M. S. Weaver, *IEEE J. Sel. Top. Quantum Electron.*, **10**, 45 (2004).
8. T. Bülow, H. Gargouri, M. Siebert, R. Rudolph, H.-H. Johannes and W. Kowalsky, *Nanoscale Res. Lett.*, **9**, 223 (2014).
9. D. Spee, K. Werf, J. Rath and R. Schropp, *Physica Status Solidi (RRL)*, **6**, 151 (2012).
10. J. Lewis, *Mater. Today*, **9**, 38 (2006).
11. S.-W. Seo, E. Jung, H. Chae, S. J. Seo, H. K. Chung and S. M. Cho, *Thin Solid Films*, **550**, 742 (2014).
12. S.-W. Seo, H. Chae, S. J. Seo, H. K. Chung and S. M. Cho, *Appl. Phys. Lett.*, **102**, 161908 (2013).
13. J. Greener, K. C. Ng, K. M. Vaeth and T. M. Smith, *J. Appl. Polym. Sci.*, **106**, 3534 (2007).